Electrodeposition of metals from supercritical fluids

Jie Ke[a], Wenta Su[a], Steven M. Howdle[a], Michael W. George[a,1], David Cook[b], Magda Perdjon-Abel[b], Philip N. Bartlett[b,1,2], Wenjian Zhang[b], Fei Cheng[b], William Levason[b], Gillian Reid[b], Jason Hyde[c], James Wilson[c], David C. Smith[c,1,2], Kanad Mallik[d], and Pier Sazio[d]

[a]School of Chemistry, University of Nottingham, Nottingham NG7 2RD, United Kingdom; Schools of [b]Chemistry and [c]Astronomy and Physics and [d]Optoelectronics Research Centre, University of Southampton, Southampton SO17 1BJ, United Kingdom

Edited by Royce W. Murray, University of North Carolina, Chapel Hill, NC, and approved June 25, 2009 (received for review February 23, 2009)

Electrodeposition is a widely used materials-deposition technology with a number of unique features, in particular, the efficient use of starting materials, conformal, and directed coating. The properties of the solvent medium for electrodeposition are critical to the technique's applicability. Supercritical fluids are unique solvents which give a wide range of advantages for chemistry in general, and materials processing in particular. However, a widely applicable approach to electrodeposition from supercritical fluids has not yet been developed. We present here a method that allows electrodeposition of a range of metals from supercritical carbon dioxide, using acetonitrile as a co-solvent and supercritical difluoromethane. This method is based on a careful selection of reagent and supporting electrolyte. There are no obvious barriers preventing this method being applied to deposit a range of materials from many different supercritical fluids. We present the deposition of 3-nm diameter nanowires in mesoporous silica templates using this methodology.

electrochemistry | nanomaterials

This paper presents a generally applicable method for electrodeposition from a homogeneous supercritical fluid (SCF). Electrodeposition is an industrially and technologically important process, with applications that range from functional and decorative coatings with precious metals through to the production of read/write heads for magnetic storage devices (1). The importance of electrodeposition is based on a number of advantageous features of the process, for instance, in precious metal plating, the efficient use of the starting material is particularly important. Electrodeposition can be used to plate curved surfaces and even inside of topologically demanding surfaces. The ability of electrodeposition to fill nano-scale features in a directed manner, that is, at, and only at, predefined locations in complex devices, is exploited in the Damascene process for the production of 20-nm width Cu interconnects within integrated circuits (ICs) (2, 3). Whilst the mass production of these small-scale features on an industrial-scale is impressive, in a research environment it is possible to electrodeposit materials on a significantly smaller-scale. This is one area where SCF based electrodeposition is likely to be particularly advantageous due to the pore penetrating ability of SCFs (4, 5).

Water is the most commonly used electrodeposition medium, and it has significant limitations due to its narrow potential window and its boiling point, which prohibits deposition above 373 K without the use of specialized techniques. These limitations have been circumvented through the use of high temperature molten salts, non-aqueous solvents, and more recently with room temperature ionic liquids (RTILs) (6). RTILs hold the advantage that they exhibit a broad electrochemical window and have opened up the electrodeposition of whole classes of technologically important materials, for example, Ge or Si (7). However, currently they are not widely used at the industrial-scale due to their high costs, lack of toxicity data, and expensive disposal/recovery (8).

SCFs provide the chemist with an alternative array of solvents that have opened the way to a range of materials and processes. SCFs exhibit properties intermediate between those of the gas and liquid states that are tuneable by temperature and pressure (9). SCFs have found many applications in extraction, fine and speciality chemistry, polymer and material modification, biotechnology and pharmaceuticals, and even in dry cleaning (10). Many of the physical properties that make these applications possible could provide benefits for electrochemical applications. Solvents such as supercritical CO_2 ($scCO_2$) also show enhanced mass transport rates and a wide electrochemical window compared to many conventional solvents. Nevertheless, there are relatively few examples of electrochemistry in SCFs. Studies that are performed in SCFs tend to focus on fundamental measurements in the so-called "active" SCFs, for example, H_2O or NH_3. Thus, there is considerable interest in understanding electrochemical corrosion mechanisms in scH_2O due to the use of supercritical and near-critical water as a coolant in nuclear reactors. Electrochemical studies in $scNH_3$ provided a route to probing the reactions, mechanisms and kinetics of the solvated electron at elevated temperatures. However, industrial applications of these approaches suffer from the aggressive nature of scH_2O and $scNH_3$, and attaining their high critical parameters.

The major problem in carrying out electrochemistry in many SCFs, such as $scCO_2$, is the non-polar nature of these solvents and the low solubility of electrolytes which results in low conductivity. The solubility of electrolytes in $scCO_2$ may be increased by adding polar co-solvents (11, 12). Alternatively, more polar SCFs, such as supercritical CH_2F_2 ($scCH_2F_2$) can be used (13).

Electrodeposition places greater demands on the working solution, electrolyte and reagent, than mechanistic or analytical electrochemical measurements; for example, a high reagent and supporting electrolyte solubility are required to allow for high deposition rates. There have been very few reports of electrodeposition from near-critical or supercritical fluids. The first work by Williams and Naiditch (14) was the deposition of Ag from near-critical and supercritical NH_3; this reaction exploited $AgNO_3$ as the reagent, which forms a co-ordination complex with the solvent, producing a stable, soluble and electro-active species. This was followed by two further studies (15, 16) of deposition from near-critical or supercritical NH_3 and H_2O. However there has not been any take up of this technique for electrodeposition. This, in part, is probably due to the aggressive nature of $scNH_3$ and the difficulties associated with generalising the method to the deposition of other materials. More recently,

Author contributions: M.W.G., P.N.B., W.L., G.R., and D.C.S. designed research; J.K., W.S., D.C., M.P.-A., W.Z., F.C., J.W., and K.M. performed research; S.M.H., W.L., G.R., and P.S. contributed new reagents/analytic tools; J.K., W.S., M.W.G., D.C., M.P.-A., P.N.B., J.H., D.C.S., K.M., and P.S. analyzed data; and M.W.G., P.N.B., and D.C.S. wrote the paper.

The authors declare no conflict of interest.

This article is a PNAS Direct Submission.

[1]To whom correspondence may be addressed. E-mail: mike.george@nottingham.ac.uk, pnb@soton.ac.uk, or d.c.smith@soton.ac.uk.

[2]P.N.B. and D.C.S. contributed equally to this work.

This article contains supporting information online at www.pnas.org/cgi/content/full/0901986106/DCSupplemental.

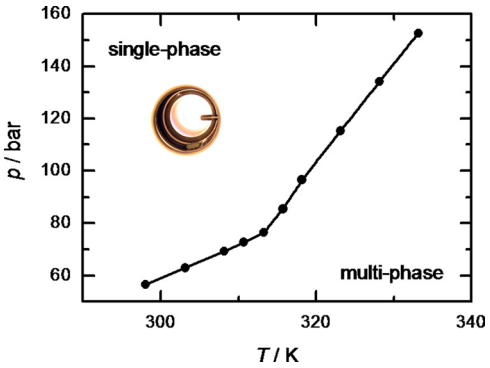

Fig. 1. Phase diagram. *P,T* phase boundary of a mixture of NBu_4BF_4 (1)+CH_3CN (2) + CO_2 (3) with $x_1 = 9 \times 10^{-4}$, $x_2 = 0.13$, and $x_3 = 0.87$. The inset photo shows a homogeneous phase of the CO_2 mixture observed inside the view-cell at the temperature and pressure in the single-phase region. The oval object sitting at the bottom of the view-cell is a magnetic stirrer bar.

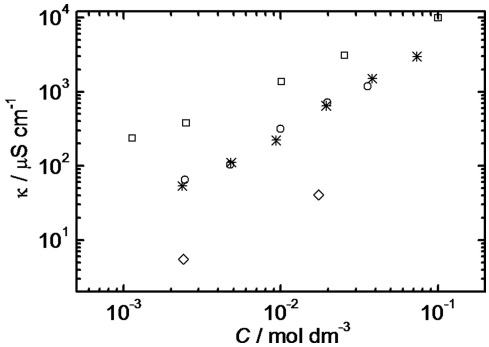

Fig. 2. Conductivity of different supercritical electrolyte solutions. Electrical conductivity of supporting electrolytes in a supercritical fluid mixture of CO_2 + CH_3CN ($x_{CO2} : x_{CH3CN} = 0.89 : 0.11$) at 328.15 K and 200 bar. Open diamonds, NBu_4BF_4; *, $[NBu_4][BARF\text{-}6]$; open circles, $[NBu_3R^f][BARF\text{-}6]$; open squares, NBu_4BF_4 in pure CH_3CN at ambient condition.

Sone and colleagues (17–20) have demonstrated the electrodeposition of nickel from an emulsion of an aqueous nickel-plating solution in $scCO_2$. This method yields smoother, higher quality Ni films than deposition from water due to the total miscibility of the H_2 evolved during the electro-deposition with $scCO_2$ (21). Unfortunately, this approach would not be suitable for electrodeposition within porous micro- or meso-porous media and also the presence of H_2O negates the advantages of the electrochemical window gained by utilizing $scCO_2$.

In this paper, we present the electrodeposition of Cu, Ag, and Co from a single-phase, above the critical point of the mixture; this is made possible by the synthesis of suitable metal complexes and a range of tailored electrolytes that permit facile electrochemistry in $scCO_2$ plus co-solvent or in $scCH_2F_2$. We also show that supercritical fluid electrodeposition can be applied to the fabrication of 3-nm metal nanowires by electrodeposition in mesoporous templates taking advantage of the low surface tension of the fluid. Our results suggest that this is a generic method which could be extended to the deposition of a wide range of materials provided the electrokinetics of deposition are favourable.

Results and Discussion

As many of the advantages of SCF electrodeposition require a homogeneous phase, we have determined the phase behavior of our working fluid. This was done using a view cell (22) to allow the phase boundary between single-phase and multiple-phase to be determined as a function of both temperature and pressure. Fig. 1 shows the results for a system containing 87.4 wt% CO_2, 12 wt% acetonitrile, and 0.6 wt% NBu_4BF_4 (corresponding to mole fractions of 0.87, 0.13, and 0.0009, respectively, and equivalent to an electrolyte concentration of 20 mM).

NBu_4BF_4 in $scCO_2$/MeCN solution shows moderate conductivity as measured using a high-pressure apparatus equipped with a modified commercial conductivity cell, see Fig. 2, and was used for the majority of the electrodeposition experiments because this electrolyte is commercially available. However higher conductivity working fluids will enable a wider range of applications. To this end, we have synthesized a number of fluorous ponytail alkylammonium cations and fluorinated tetraphenylborates (23), which are designed to be more soluble in our low dielectric coefficient SCFs. Fig. 2 shows conductivity data for some of these electrolytes in $scCO_2$/MeCN. In the case of the best systems such as $NBu_4BARF\text{-}6$ (BARF-6 = $[B\{3,5\text{-}(CF_3)_2C_6H_3\}_4]^-$, see SI for structures) the conductivity is an order of magnitude higher than that for the parent NBu_4BF_4. These represent the most conducting solutions with $scCO_2$ reported to date with the conductivity of $NBu_4BARF\text{-}6$ (19.5 mM) in $scCO_2$/MeCN (13 vol/vol%) being 648 μS cm^{-1} at 55 °C and 200 bar. These data can be compared to those reported for tetrakis(decyl)ammonium tetraphenylborate (19.2 mM) in pure $scCO_2$ at 70 °C and 300 bar (κ = 1.7 μS cm^{-1}) (24) and for $LiCF_3CO_2$ (23 mM) in $scCO_2$/MeOH mixture (23 vol/vol%) at 32 °C and 69 bar (κ = 250 μS cm^{-1}) (11). Our $scCO_2$/MeCN mixture has 2–3 times higher conductivity than the $scCO_2$/MeOH system. This conductivity is achieved with considerably less co-solvent, which is important because the properties of the mixture are a composition weighted average between those of the SCF and the co-solvent and so our mixture retains more of the advantages of a SCF.

Fig. 3 shows representative cyclic voltammogram for $[Cu(MeCN)_4]BF_4$ in 87.4 wt% CO_2, 12 wt% acetonitrile, 0.6 wt% NBu_4BF_4. In a series of separate experiments, we confirmed that addition of the copper salt up to saturation did not significantly alter the fluid-liquid phase boundary of the system and that at 36–38 °C and 172 bar we have a single supercritical fluid. The voltammetry shows the expected form with mass transport limited reduction of Cu(I) to Cu(0) at negative potentials, accompanied by a stripping peak for Cu on the return scan. The stripping peak is sharp and undistorted, showing that IR drop is insignificant in these experiments. The faradaic efficiency for Cu deposition was calculated by comparing the charge passed to deposit Cu to the charge passed for Cu stripping

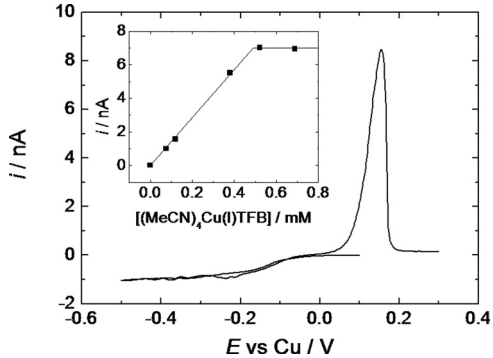

Fig. 3. Copper voltammetry. Copper voltammetry was performed in $scCO_2$ with 12.1 wt % MeCN and NBu_4BF_4 (20 mM); at 37 °C and 172.4 bar. Electrodes were: 25 μm diameter platinum disc working electrode, 0.5 mm diameter platinum disc pseudo reference, and 0.5 mm diameter platinum wire counter electrode. The sweep rate was 20 mV s^{-1}.

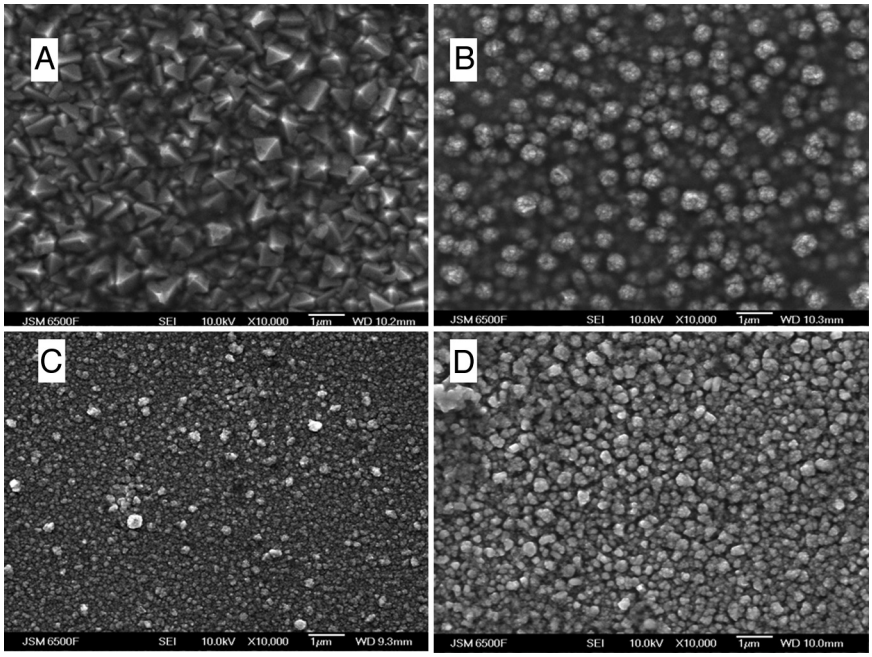

Fig. 4. Electroplated copper SEM images of copper films deposited from a saturated solution of $[Cu(MeCN)_4]BF_4$ in 87.4 wt% CO_2, 13 wt% acetonitrile, 0.6 wt% NBu_4BF_4 36–38 °C and 138 bar at (*A*) −0.6 V, (*B*) −0.9 V, (*C*) −1.5 V, and (*D*) −1.7 V vs. Pt.

and was found to be 50–60% at the microdiscs and >95% at the larger electrodes.

The inset in Fig. 3 shows a plot of the mass transport limited currents recorded at a microdisc electrode for different concentrations of $[Cu(MeCN)_4]BF_4$ added to the solution. At low $[Cu(MeCN)_4]BF_4$ concentrations the current increases linearly with the concentration and from the slope, using the microdisc equation (25), we obtain a diffusion coefficient of 3.5×10^{-5} cm^2 s^{-1} in the supercritical fluid. This is approximately 1.6-times larger than the value measured for the same complex in acetonitrile at 38 °C (2.2×10^{-5} cm^2 s^{-1}). At high $[Cu(MeCN)_4]BF_4$ concentrations (Fig. 3 inset) the limiting current reaches a plateau value indicating that the solution is now saturated. From the intersection of the original linear portion and the plateau we obtain an estimate of the solubility of $[Cu(MeCN)_4]BF_4$ in the supercritical fluid under these conditions of 0.49 mM. It is interesting to note that by changing the anion we can significantly increase the solubility of the $[Cu(MeCN)_4]^+$ complex. Thus when we use 87.4 wt% CO_2, 12 wt% acetonitrile, and 0.6 wt% NBu_4BARF-6, the solubility is increased more than 30-fold with a corresponding diffusion coefficient of 4.5×10^{-5} cm^2 s^{-1}. This illustrates another significant advantage of careful choice and design of the electrolyte to enhance electrodeposition from supercritical fluids.

Similar results were obtained for the deposition of Ag and Co from the corresponding acetonitrile complexes, $[Ag(MeCN)_4]BF_4$ and $[Co(Me(CN)_6][BF_4]_2$ in the same supercritical solution. Although it is also possible to deposit copper and silver from other complexes in this supercritical solution in these cases there were always complications due to electrode fouling and/or side reaction of the ligands which limited the process. The acetonitrile complexes have the advantage of not introducing any additional ligands to the solution which might lead to competing reactions at the cathode or unwanted side products at the anode.

To demonstrate that this general approach can be extended to other supercritical fluids we have carried out electrodeposition of Cu from $[Cu(MeCN)_4]BF_4$ in $scCH_2F_2$ (R32). $scCH_2F_2$ has a higher dielectric constant than $scCO_2$ so a co-solvent is not required and high conductivities are achievable given the correct choice of electrolyte [e.g., NBu_4BF_4 (20 mM) has a conductivity of 2.3 mS cm^{-1} in CH_2F_2 at 90 °C and 260 bar]. Supercritical fluorinated hydrocarbons, such as $scCH_2F_2$, also offer the advantage of a wider potential window, and indeed Abbott has shown that xenon can be oxidised in supercritical CF_3CH_2F (R134a) (26). In our experiments, copper was deposited from a $scCH_2F_2$ solution containing 0.104 wt% $[Cu(MeCN)_4]BF_4$, 0.626 wt% NBu_4BF_4 at 89 °C (≈11 °C above the critical temperature of CH_2F_2) and 114 bar. The resulting cyclic voltammograms were similar to that shown in Fig. 3 with clear evidence of both a nucleation loop and a stripping peak.

To demonstrate that this approach can be used to deposit bulk metal samples, we have plated Cu onto macroscopic (0.4 to 1 cm^2) evaporated gold on glass electrodes. In this case the deposition was carried out from a saturated solution of $[Cu(MeCN)_4]BF_4$ in 87.4 wt% CO_2, 13 wt% acetonitrile, 0.6 wt% NBu_4BF_4 under potentiostatic conditions and at 138 bar. The currents increase for the first 5,000 s and then stabilize with a deposition current density of around 17 μA cm^{-2} corresponding to a deposition rate of 45 nm h^{-1}.

The morphology of the deposits varies with the applied potential as expected, Fig. 4. At high overpotentials, when the deposition is mass transport limited, the films are rough and dendritic, whereas at low overpotentials smooth, shiny, adherent films which tarnish rapidly on contact with air are obtained. EDX, SIMS, and Auger studies all show that the films are high purity copper.

Four-point probe measurements gave film resistivities for the best films of 4×10^{-6} Ω cm, which is comparable to values reported for copper electrodeposition from aqueous solution [1.75 to 2×10^{-6} Ω cm depending on plating bath additives Vas'ko et al. (27)] or by chemical deposition in supercritical CO_2 as reported by Watkins et al. (28) (2×10^{-6} Ω cm). Thus, there is no evidence of significant incorporation of impurities from the plating bath into the deposits and their quality is high and close to that required for device applications.

When the NBu_4BARF-6 electrolyte and 2.29 mM $[Cu(MeCN)_4]$BARF-6 were used much higher deposition currents were obtained (82 μA cm^{-2}, maximum plating rate 220 nm

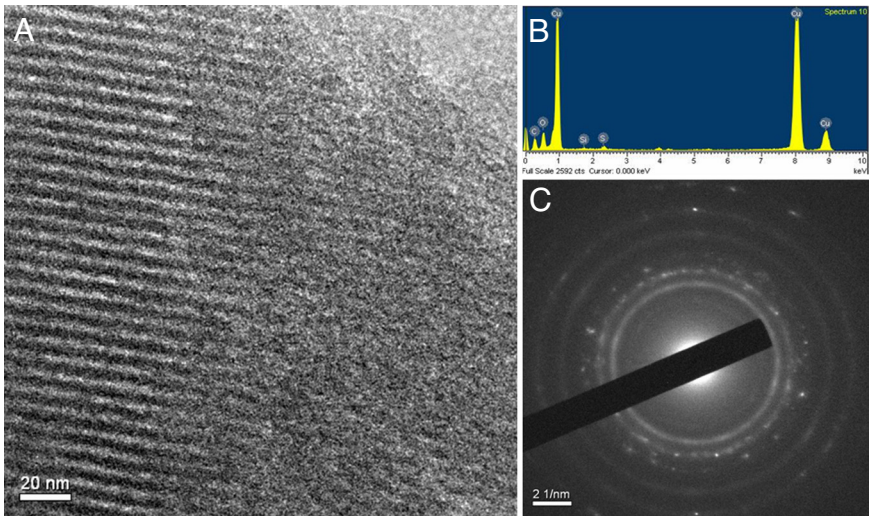

Fig. 5. Copper nanorods in mesoporous silica. (*A*) TEM of copper nanorods electrodeposited into silica mesopores from a solution of SC CO_2 with 12.1 wt % MeCN, 20 mM $[NBu_4][BARF\text{-}6]$, and 2 mM $[Cu(MeCN)_4][BARF\text{-}6]$ at 38 °C and 172.4 bar. The working electrode was a 0.8 × 0.5 cm ITO on glass slide modified with approximately 250 nm thick film of mesoporous silica; the counter electrode was a large, coiled, copper wire and the reference electrode was a 0.5-mm diameter copper disc. (*B*) EDX spectrum recorded from the same TEM sample. (*C*) Selected area electron diffraction (SAED) pattern recorded on 1 of the copper rods.

h^{-1}) as a result of the greater solubility of the copper complex, but again high quality, shiny, adherent films of metallic copper were produced.

Finally, to demonstrate the application of this approach to the deposition of metal into nanoscale (< 10 nm) pores we investigated the electrodeposition of copper from the supercritical solution into nanostructured mesoporous silica templates. The templates were prepared by dip coating ITO slides in a solution of Brij56:TMOS:0.5 M HCl:MeOH (1:1.8:1:3.8 by weight). After calcining at 350 °C under N_2 for 4 h to remove the surfactant, this produces an adherent mesoporous silica film roughly 200 nm thick on the ITO surface containing a regular hexagonal array of approximately 3-nm diameter cylindrical pores approximately 6 nm apart as shown by SAXS and TEM studies (see SI). These mesoporous silica coated electrodes were cut into pieces 0.3–1.0 cm^2, contacted to a platinum wire with silver paint and insulated with epoxy resin. Electrochemical deposition of copper was carried out from the $scCO_2$/MeCN at −0.4 V vs. Cu to pass a total charge of 67 mC cm^{-2}. This charge was calculated to be sufficient to substantially fill all of the exposed mesopores. After deposition, the electrodes were rinsed with acetone and distilled water and samples examined by TEM. Fig. 5*A* shows a typical TEM image of the sample. The regular array of cylindrical pores is clearly visible in cross section on the left hand side of the image, the average pore diameter and separation are 3 nm and 6 nm. Evidence that the pores are filled with copper is provided by the EDX analysis, which shows strong copper as well as the expected silicon and oxygen signals, Fig. 5*B*, and by the selected area electron diffraction results, Fig. 5*C*, which show a combination of diffuse rings attributed to silica together with rings that are consistent with the expected (111), (200), (220), and (311) diffraction peaks for copper.

The experiments reported here show that, by the appropriate selection of the anion and cation, it is possible to have significant electrical conductivity from supercritical fluid electrolytes (>1 mS cm^{-1}) from either CO_2/MeCN or from CH_2F_2. These fluids are supercritical at modest temperatures and pressures (less than 100 °C and 200 bar) and as such that they can be readily used in electrochemical studies. Furthermore, we have shown that selection of an appropriate metal complex containing a ligand set which does not interfere with the electrochemistry and provides sufficient solubility in the supercritical electrolyte allows the electrochemical deposition of high quality, adherent metal films from both supercritical CO_2/MeCN and supercritical CH_2F_2. Using this approach we have shown that we can grow 3-nm diameter copper nanowires by electrodeposition into the pores of a nanostructured mesoporous silica template. These results demonstrate that electrodeposition from supercritical solution is an attractive approach to the fabrication of nanostructured materials at the sub 10-nm scale where we take advantage of the control offered by the electroplating process and combine this with the low surface tension, extended potential window and possible elevated temperature deposition offered by the supercritical fluid.

Materials and Methods

The cell used for the electrochemistry was a 2-piece stainless steel construction. The bottom part has a 10-mL well (that constitutes the working volume when assembled) and the top has 7 $^1/_{16}$,'' female, SSI type fittings (through which electrodes, thermocouples and tubing could be sealed into the cell) and 1 unique safety valve. The 2 pieces are fitted together using a disposable elastomeric O-ring and a clamp that is locked in place.

Electrolytes and metal complexes were introduced into the cell either as dry powders or solutions in acetonitrile. This loading step was carried out in a dry, dinitrogen-purged glove box when air sensitive materials were used. For the experiments in $scCO_2$/acetonitrile mixture the cell was preheated to the desired temperature using a band heater under PID control and supercritical fluid grade CO_2 (99.9995%, BOC) was then added via a specialized CO_2 delivery pump (PU-1580-CO_2, JASCO). CO_2 was pumped at rates from 0.1–1.0 mL min^{-1} (to ensure that the cell temperature remained constant) until the desired pressure and CO_2:acetonitrile ratio was achieved. The system was also stirred during pumping, using a magnetic stirrer, to ensure the solution was homogeneous. Stirring was stopped at least 5 min before any electrochemical measurements to allow the solution to settle.

For the CH_2F_2 experiments, the solvent was condensed into the cell from a pressurized sampling cylinder. To do this the cell (already loaded with dry electrolyte and metal complexes) was cooled to −10 °C using dry ice. The amount of CH_2F_2 added to the cell was calculated by weighing the sampling cylinder before and after. Once the solvent has been added the cell is heated to the desired temperature while monitoring the pressure. Again the solution is stirred to ensure homogeneity except during electrochemical measurements.

Cyclic voltammetry and chronoamperometry were performed using 2 potentiostats (Autolab, AUT72613, Windsor Scientific, and PARSTAT 2273, Princeton Applied Research).

Working electrodes were: evaporated gold slides (microscope slides with a 15-nm chromium adhesion layer and 100 nm gold); 0.5-mm diameter platinum

discs (sealed into $^1/_{16}$'' O.D. PEEK tubing) or platinum microdiscs (7.5, 25, 33, and 50 μm diameter) sealed in glass. Counter electrodes were: 0.5-mm diameter platinum, silver or copper wires (sealed into $^1/_{16}$'' O.D. PEEK tubing). Reference electrodes were: 0.5 mm diameter platinum, silver or copper discs (sealed into $^1/_{16}$'' O.D. PEEK tubing). The counter and reference electrodes were usually chosen to match the metal complex in solution. This has the advantage that the copper or silver disc forms a stable reference by exchanging ions with the solution, while the copper or silver wire can oxidize during metal plating thus providing a suitable equivalent reaction to balance the electrochemistry at the working electrode.

Phase behavior of the supercritical solutions was studied using a variable volume view cell that was purpose built at the University of Nottingham. The detailed description of the apparatus and the experimental procedure can be found elsewhere (22).

For electric conductivity measurements, the front window of the view cell was replaced with a steel electrode holder. Two pieces of platinum foils (0.4 cm^2 each) were mounted to the inner surface of a glass tube that was attached to the electrode holder. The conductivity measurements were made with JENWAY 4510 conductivity meter, and the cell constant was calibrated using the standard conductivity solutions of KCl. The conductivity measurements were only carried out under the conditions corresponding to a homogeneous single phase present in the cell.

Mesoporous silica substrates were prepared on ITO coated glass slides using a method adapted from that described by Attard et al. (29) The slides were first cleaned by sonicating in a solution of 50 vol% acetone in deionized water (1 h). Slides were then etched in 5 M KOH for 2 h (to generate a hydroxyl functionalized surface); rinsed with deionized water and ethanol and then dried with a flow of argon before dip coating with the silica templating mixture. The templating mixture consisted of Brij 56, TMOS, 0.5 M HCl, and methanol in the ratio of 1:1.8:1:3.8 by weight. The surfactant, TMOS and methanol were mixed at 45 °C and the polymerization of TMOS was initiated by the addition of HCl. Once the ITO slides were dip-coated with the templating mixture they were dried, in air, at 45 °C for 3 days before calcination at 350 °C under nitrogen for 4 h. Finally the templated ITO slides were cooled for 6 h in air.

Tetrabutylammonium tetrafluoroborate and tetrakis-acetonitrile silver(I) tetrafluoroborate were both purchased from Aldrich and used without further purification. R32 was supplied by Ineous Fluor and was dried and cleaned, by passing over 4-Å molecular sieves and activated charcoal, before use. Acetonitrile was purchased from Fisher Scientific (99.98%) and distilled over CaH_2 before use. All other complexes and electrolytes were synthesised at the University of Southampton. Details of the synthesis and characterization of all compounds are to be published elsewhere.

ACKNOWLEDGMENTS. We wish to acknowledge M. Poliakoff for useful discussions and P. Fields and R. Wilson for technical support. M.W.G. gratefully acknowledges receipt of a Royal Society Wolfson Merit Award. The work presented here was funded by Research Council, United Kingdom via a Basic Technology Grant.

1. Schlesinger M, Paunovic M (2000) in *Modern Electroplating* (Wiley, New York).
2. Andricacos PC, Uzoh C, Duckovic, JO, Horkans J, Deligianni H (1998) Damascene copper electroplating for chip interconnects. *IBM J Res and Dev* 42:567–574.
3. Fukami K, Tanaka Y, Chourou ML, Sakka T, Ogata YH (2009) Filling of mesoporous silicon with copper by electrodeposition from an aqueous solution. *Electrochim Acta* 54:2197–2202.
4. Verkerk AW, Goetheer ELV, van den Broeke LJP, Keurentjes JTF (2002) Permeation of carbon dioxide through a microporous silica membrane at subcritical and supercritical conditions. *Langmuir* 18:6807–6812.
5. Dickson JL, Gupta G, Horozov TS, Binks BP, Johnston KP (2006) Wetting phenomena at the CO_2/water/glass interface. *Langmuir* 22:2161–2170.
6. Abbott AP, McKenzie KJ (2006) Application of ionic liquids to electrodeposition of metals. *Phys Chem Chem Phys* 8:4265–4279.
7. Al-Salman R, Zein El, Abedinw S, Endres F (2008) Electrodeposition of Ge, Si and Si_xGe_{1-x} from an air- and water-stable ionic liquid. *Phys Chem Chem Phys* 10:4650–4657.
8. Romero A, Santos A, Tojo J, Rodriguez A (2008) Toxicity and biodegradability of imidazolium ionic liquids. *J Hazard Mater* 151:268–273.
9. Clifford T (1999) in *Fundamentals of Supercritical Fluids* (Oxford Univ Press, Oxford).
10. Jessop PG, Leitner W. (1999) in *Chemical Synthesis Using Supercritical Fluids* (Wiley-VCH, Chichester).
11. Jun J, Fedkiw PS (2001) Ionic conductivity of alkali-metal salts in sub- and supercritical carbon dioxide + methanol mixtures. *J Electroanal Chem* 515:113–122.
12. Wu WZ, et al. (2003) Solubility of room-temperature ionic liquid in supercritical CO_2 with and without organic compounds. *Chem Commun* 1412–1413.
13. Abbott AP, Eardley CA (2000) Conductivity of $(C_4H_9)_4N$ BF_4 in liquid and supercritical hydrofluorocarbons. *J Phys Chem B* 104:9351–9355.
14. Williams RA, Naiditch S (1970) Electrodeposition of silver from dense gaseous solutions of silver nitrate in ammonia. *Phys Chem Liq* 2:67–75.
15. McDonald AC, Fan FRF, Bard AJ (1986) Electrochemistry in near-critical and supercritical fluids. *J Phys Chem* 90:196–202.
16. Silvestri G, Gambino S, Filardo G, Cuccia C, Guarino E (1981) Electrochemical processes in supercritical phases. *Angew Chem Int Edit* 20:101–102.
17. Yan H, Sone M, Sato N, Ichihara S, Miyata S (2004) The effects of dense carbon dioxide on nickel plating using emulsion of carbon dioxide in electroplating solution. *Surf Coat Technol* 182:329–334.
18. Yoshida H, et al. (2002) Electroplating of nanostructured nickel in emulsion of supercritical carbon dioxide in electrolyte solution. *Chem Lett* 1086–1087.
19. Yoshida H, et al. (2003) Application of emulsion of dense carbon dioxide in electroplating solution with nonionic surfactants for nickel electroplating. *Surf Coat Technol* 173:285–292.
20. Yoshida H, et al. (2004) New electroplating method of nickel in emulsion of supercritical carbon dioxide and electroplating solution to enhance uniformity and hardness of plated film. *Thin Solid Films* 446:194–199.
21. Howdle SM, Bagratshvili VN (1993) The effects of fliud density on the rotational Raman-spectrum of hydrogen dissolved in supercritical carbon-dioxide. *Chem Phys Lett* 214:215–219.
22. Licence P, et al. (2004) Large-aperture variable-volume view cell for the determination of phase-equilibria in high pressure systems and supercritical fluids. *Rev Sci Instrum* 75:3233–3236.
23. LeSuer RJ, Buttolph C, Geiger WE (2004) Comparison of the conductivity properties of the tetrabutylammonium salt of tetrakis(pentafluorophenyl)borate anion with those of traditional supporting electrolyte anions in nonaqueous solvents. *Anal Chem* 76:6395–6401.
24. Abbott AP, Harper JC (1996) Electrochemical investigations in supercritical carbon dioxide. *J Chem Soc Faraday Trans* 92:3895–3898.
25. Bard AJ, Faulkner LR (2001) in *Electrochemical Methods: Fundamentals and Applications* (John Wiley and Sons, New York).
26. Abbott AP, Eardley CA, Harper JC, Hope EG (1998) Electrochemical investigations in liquid and supercritical 1,1,1,2,-tetrafluoroethane (HFC 134a) and difluoromethane (HFC 32). *J Electroanal Chem* 457:1–4.
27. Vas'ko VA, Tabakovic I, Riemer SC, Kief MT (2004) Effect of organic additives on structure, restivity and room temperature recrystallization of electrodeposited copper. *Microelectron Eng* 75:71–77.
28. Cabanas A, Shan X, Watkins JJ (2003) Alcohol-assisted deposition of copper films from supercritical carbon dioxide. *Chem Mater* 15:2910–2916.
29. Attard GS, Glyde JC, Goltner CG (1995) Liquid-crystalline phases as templates for the synthesis of mesoporous silica. *Nature* 378:366–368.